EF3 COL 2.0-28-A

2.5.3 Surface Faulting

Subsection 2.5.3 contains an evaluation of the potential for tectonic and nontectonic surface deformation at the Fermi 3 site. Information contained in this subsection, which was developed in accordance with Regulatory Guides 1.165 and 1.208, is intended to demonstrate compliance with 10 CFR 100.23, Geologic and Seismic Siting Criteria.

This subsection contains the following information:

- Potential surface deformation associated with capable tectonic sources.
- Potential surface deformation associated with nontectonic processes, such as glaciotectonic deformation, unloading (pop-ups), subsurface salt migration (salt domes), growth faults, dissolution and collapse (karst-related), volcanism, and man-induced deformation (e.g., mining collapse, subsidence due to fluid withdrawal).

The conclusions regarding the potential for surface deformation are summarized as follows:

- There are no capable tectonic fault sources within the site area (8-km [5-mi] radius) or vicinity (40-km [25-mi] radius). A capable tectonic source, as defined by Regulatory Guide 1.208, is a tectonic structure that can generate both vibratory ground motion and tectonic surface deformation, such as faulting or folding at or near the earth's surface in the present seismotectonic regime. There is no evidence of Quaternary tectonic surface faulting or fold deformation within the Fermi 3 site location (1-km [0.6-mi] radius).
- The potential for nontectonic deformation at the site is negligible.

The following subsections provide the data, observations, and reference citations to support these conclusions.

2.5.3.1 Geological, Seismological, and Geophysical Investigations

Information regarding the potential for surface faulting at the Fermi 3 site is documented in the following sources:

- Previous site investigations described in the Fermi 2 UFSAR, Section 2.5 (Reference 2.5.3-201)
- Published and unpublished literature and data on structures and tectonics in southeast Michigan and northwest Ohio as discussed in Subsection 2.5.1.1.4 and Subsection 2.5.1.2.4

- Seismicity data compiled and analyzed in publications and the updated seismicity catalog (Subsection 2.5.2.1)

Additional investigations performed to assess the potential for future surface faulting and related deformation at the Fermi 3 site and surrounding site area included the following:

- Compilation and review of available site area data, with an emphasis on reports and information published since the original geologic investigation for the Fermi 2 FSAR and site–specific information collected for the Fermi 3 COLA. Mapped bedrock structures in the site vicinity are shown on Figure 2.5.3-201.
- Interpretation of aerial photographs and remote sensing imagery. The most detailed topographic data available for the site vicinity (40-km [25-mi] radius from the site) is the UGSG 10-m digital elevation model (DEM). A shaded relief model created using the DEM was used to conduct a visual lineament analysis for the site vicinity. In the site area (within the 8-km [5-mi] radius) U.S. Department of Agriculture (USDA) 1:20,000-scale, black and white photos from 1955 also were used in field reconnaissance and to aid in identifying potential lineaments. Color infrared aerial photographs with a two meter resolution of the site location also were used to identify lineaments. Observations based on the lineament analyses are discussed in Subsection 2.5.3.2.3.
- Field and aerial reconnaissance. Field investigations were conducted during August 2007, and involved consultations and field trips with local experts, examination of known faults in the site vicinity, examination of well-documented exposures of stratigraphic units as described in previous publications, examination of exposures in quarries, and aerial (helicopter) reconnaissance. Figure 2.5.3-202 shows field localities visited and the helicopter reconnaissance route.
- Discussions with current researchers in the area. Local experts from the Ohio Geological Survey, the Michigan Geological Survey, the Geological Survey of Canada, and the Ontario Geological Survey were contacted to obtain the latest available information relevant to the site geology and tectonics of the region.

2.5.3.2 Geological Evidence, or Absence of Evidence, for Surface Deformation

2.5.3.2.1 Tectonic Deformation

Based on a review of published literature and maps and field reconnaissance in the site area, there are no faults at or near the ground surface in Quaternary glacial or lacustrine sediments within 40-km (25-mi) of the site. The Fermi 2 UFSAR also concluded, based on a review of available literature, conferences with geological organizations, and onsite investigations, that no known faults exist within 40-km (25-mi) of the Fermi 2 site and that there are no capable faults within 320-km (200-mi) of the site.

No Quaternary faults are known within the site vicinity based on review of more recent publications and data, interpretation of remote sensing imagery (10-m DEM and 1:20,000 aerial photographs) and observations from field and aerial reconnaissance. Review of available data and published interpretations of boring and geophysical data obtained primarily from oil and gas exploration indicates, however, that faults are present within Paleozoic rocks in the subsurface in the site vicinity. The location of known and postulated structures within the site vicinity is shown on Figure 2.5.3-201 and discussed in Subsection 2.5.1.2.4. The Bowling Green fault and the Maumee fault are subsurface bedrock faults mapped within 40-km (25-mi) of the site (Figure 2.5.1-246). The Howell anticline and associated fault, is mapped to within 45-km (28-mi) of the site. A series of folds are recognized in subsurface bedrock units along the southeastern projected trend of the Howell anticline/fault structure. Two poorly documented possible fault trends, associated with the New Boston and Sumpter oil and gas pools, are postulated along the southwestern flank of this series of folds (Figure 2.5.1-203, Figure 2.5.1-230). Additional shorter faults are mapped in southwestern Ontario, including two subparallel unnamed faults, one of which is associated with the Colchester oil and gas field. A summary of the evidence for the location, timing, and displacement on these structures is provided in Subsection 2.5.1.2.4.1 and Table 2.5.1-201.

Only one possible fault, the fault trend associated with the New Boston pool as mapped in a 1962 publication by Ells (Reference 2.5.3-202), extends within the site area (8-km [5-mi] radius). However, as discussed in Subsection 2.5.1.2.4.1, there is no documentation supporting the existence of this postulated structure; the location is known only from a

small scale map (approximately one inch = 60 miles) (Reference 2.5.3-202). The folds, which are defined based on structure contours on the top of the Ordovician Trenton Formation (Figure 2.5.1-247), have gently dipping limbs (less than 0.9 degrees) and there is nothing in the character of the folds that suggests the folds are fault-cored. The folds are not well expressed in the structure contours on the Trenton Group as illustrated on Figure 2.5.1-248a. Ells does not show these postulated fault trends along the New Boston and Sumpter oil pools on his more recent compilation of fault or fold structures (Reference 2.5.3-203).

The shallow-dipping northwest-southeast-trending synclinal fold identified based on subsurface investigations for the Fermi 2 site (Reference 2.5.3-201) and confirmed by additional Fermi 3 borings (Figure 2.5.1-237 and Figure 2.5.1-249) has a similar orientation to the other fold trends observed in Devonian bedrock units to the north of the site (Figure 2.5.1-247). These minor folds may be third-order structures that are structurally related to the distal end of the Howell anticline/fault structure as it dies out to the southeast. These minor folds and postulated faults are assumed to be comparable in age to the Howell anticline/fault structure, which is older than late Mississippian (Subsection 2.5.1.1.4.3.2.9).

Faults were not identified within the basement rocks or overlying sedimentary strata at the Fermi 2 site (Reference 2.5.3-201). As noted in the Fermi 2 UFSAR, competent bedrock strata were shown to underlie the site and there are no major solution cavities or zones of solution weathering in the site area. Subsequent to blasting operations during excavation of the Fermi 2 site, the exposed foundation bedrock was sluiced with high-pressure water jets and carefully examined by a qualified geologist to ensure that no excessive natural fracturing or blasting back-break existed that might be unsuitable for foundation support (Reference 2.5.3-201).

2.5.3.2.2 Nontectonic Deformation

Various glacial and periglacial processes may create geomorphic features that mimic surface tectonic fault rupture. The various types of faults observed in glaciated regions are classified into the following categories: (Reference 2.5.3-204)

- **Glacio-isostatic** (commonly referred to as postglacial) faulting that occurs in regions of ice cover in response to changes in the glacial load, either as a result of deglaciation (crustal unloading) or glacial advance (crustal loading)
- **Glaciotectonic** faulting used to denote any deformation resulting from ice movement (ice push or ice drag)
- **Periglacial** faulting resulting from freeze-thaw processes
- **Shallow stress-relief** faulting resulting in formation of pop-up structures. Shallow stress-relief structures due to glacial loading/unloading will be spatially and temporally associated with the extent and timing of glaciers. Shallow stress-relief faulting also can result from non-glacial unloading mechanisms, both natural (i.e., erosion) and cultural (i.e., quarrying). Both mechanisms result from the relief of shallow stress in the regional compressive stress regime.

A summary of the characteristics of these types of structures and criteria for differentiating them from tectonic surface faulting is provided in Hanson et al. (Reference 2.5.3-204).

No evidence of surface deformation related to any of these mechanisms has been reported in the publications reviewed or was observed in the site area during the field reconnaissance investigation. Subsection 2.5.1.1.3.3 of the Fermi 2 UFSAR and Subsection 2.5.1.2.6.3 of the Fermi 3 FSAR state that actual pop-ups have not been noted in southeastern Michigan or adjacent portions of Ohio, Indiana, or Canada, but surficial folding of Devonian shales has been observed in northwestern Ohio. During the excavation process for Fermi 2, no rockbursts, pop-ups, or heaves were seen. This was attributed to a lack of compressive stresses and insufficient depth of excavation to reduce lithostatic loading sufficiently to cause such features to occur (Reference 2.5.3-201).

Other nontectonic mechanisms that have produced surface deformation, recognized elsewhere in the Michigan Basin region, are related to dissolution of carbonate rock leading to collapse and subsidence and dissolution and movement of salt bodies. Karst related problems have been reported for the (320-km [200-mi] radius) site region; in northwestern Ohio and adjacent Indiana and southeastern Michigan karst occurs in Silurian-age limestones and dolomites. As noted in Subsection 2.5.1.1.5, certain problems have been identified in

northwestern Ohio where the carbonate rocks are covered by less than 6 m (20 ft) of glacial deposits. Evaporative karst (karst in halite or gypsum deposits) occurs in the central portion of the Michigan Basin. However, as noted in Subsection 2.5.1.2.6.7.3, no salt deposits exist in the (8-km [5-mi] radius) site area. Based on descriptions of voids and soft rock conditions encountered in the Fermi 2 borings (Reference 2.5.3-201) and Fermi 3 borings (Subsection 2.5.1.2.3), no major solution cavities or zones of solution weathering were encountered during subsurface investigations at the Fermi site.

2.5.3.2.3 Results of Lineament Analyses

Faults and fractures can be expressed at the surface in a variety of ways, including regional lineaments, linear drainage lines, abrupt or anomalous changes in stream direction, vegetation changes, soil changes, changes in drainage density, abrupt topographic changes or scarps, and changes in land use. Lineaments can also be nontectonic in origin, relating to differential erosion, beach ridge formation, soil-type changes related to stratigraphic facies variations, and cultural features. Two different types of remote sensing imagery were used to identify lineaments in the site vicinity and site area. Hillshade models, based on the USGS 10-m digital elevation model (DEM), were used to identify topographic and linear stream segments in the site vicinity. Interpreted and uninterpreted hillshade model maps are shown on Figure 2.5.3-203 and Figure 2.5.3-204, respectively. Within the 8-km (5 mi) site area, 1:20,000-scale black and white stereo aerial photograph pairs also were interpreted. Interpreted and uninterpreted aerial photograph mosaics are shown on Figure 2.5.3-205 and Figure 2.5.3-206, respectively. Lineaments identified in the 1955 aerial photographs were also compared to more recent color infrared aerial photographs of the site location (Figure 2.5.3-207 and Figure 2.5.3-208). Figure 2.5.3-209 presents recent color infrared aerial photographs for the site location.

As shown on Figure 2.5.3-203, there are numerous topographic lineaments in the site vicinity that are evident on hillshade models derived from the USGS 10-m DEM. Most of the lineaments either coincide with linear stream segments or are shore-parallel lineations that appear to coincide with mapped paleo-shoreline features as shown on (designated by n_1, n_2, and n_3 on Figure 2.5.3-203). The majority of the lineaments generally trend N30W to N60W. Other trends are E-W, N-S, N30E, and N70E. These trends are consistent with regional joint and fracture trends

described in Subsection 2.5.1.2.4.3. The dominant trends of joints in the Bass Islands Group are N45° to 60°W and N40° to 50°E and are nearly vertical in dip (Reference 2.5.3-201). Mapping of the excavation for the Fermi 2 reactor/auxiliary building indicated trends of N45° to 60°W and N60° to 50°E.

Many of the lineaments parallel the trend of the Howell Anticline, N40° to 60°W. The subsurface Sumpter Pool and New Boston Pool possible faults (Reference 2.5.3-202) located to the north and west of the site also trend approximately N40W. However, with the possible exception of the possible Sumpter Pool fault, none of the identified structures directly coincide with the identified lineaments and there is no geomorphic evidence of recent surface deformation along any of the identified or postulated structures. Paleo-shoreline features, beach ridges, cross the trend of the postulated Sumpter Pool and New Boston field possible fault trends with no apparent disruption (n_1 on Figure 2.5.3-201). The actual channels of the drainages are very sinuous and appear to follow both northwest- and northeast-trending fracture and joint trends observed in bedrock elsewhere in the site area. However, bedrock in the site area generally is mantled by several meters of Quaternary glacial and glacio-lacustrine sediments, and it is not clear that present drainage channels are controlled by bedrock structure. Glacial (subglacial meltwater channels) and post-glacial shoreline features also may have influenced present drainage patterns.

The site area lies east of a series of paleo shorelines that post-date the last glacial epoch. Therefore, the surficial deposits and geomorphic surfaces in the site area are younger than about 13,000 years. Given the low strain rates in the site region, the young surficial and near surface deposits are unsuitable for detecting long-term neotectonic strain deformation. Despite these limitations, the USDA 1:20,000-scale color stereo photographs were examined to assess whether or not any significant structural trends could be identified. As shown on Figure 2.5.3-205, there are several WNW- to NNW-trending lineaments in the site area. The lineaments generally consist of aligned linear features that include linear tonal contrasts, linear drainages, linear breaks in slope (e.g., the back edges of flood plains and alluvial terraces). The observed trends are consistent with the trends of the topographic lineaments identified in the site vicinity (Figure 2.5.3-203) and the lineaments are inferred to be the result of surficial erosional processes. The near-surface

deposits are too young to provide a useful means for assessing fault capability. Nonetheless, no evidence was observed that would indicate the presence of post-glacial surface faulting or ongoing tectonic deformation.

2.5.3.3 Correlation of Earthquakes with Capable Tectonic Sources

There have been no historically reported earthquakes or alignments of earthquakes within 40-km (25-mi) of the site that can be associated with a mapped bedrock fault (Subsection 2.5.2.1 and Figure 2.5.1-203).

2.5.3.4 Ages of Most Recent Deformations

The major deformation on bedrock structures in the site vicinity appears to have occurred during the Paleozoic and most faults in the region are believed to have been dormant since late Paleozoic time, at least 200 million years ago (Reference 2.5.3-201; Figure 2.5.1-201 and Subsection 2.5.1.1.4.3). Earthquakes in the region are generally shallow events associated with reactivated Precambrian faults favorably oriented in the modern northeast-southwest compressive stress regime (Reference 2.5.3-205, Reference 2.5.3-206). None of these events has associated surface rupture, and no faults in the site region exhibit evidence of movement since the Paleozoic. Evidence for Mesozoic extension resulting in reactivation of Precambrian rifts is present in the Mississippi embayment and the St. Lawrence Valley system, but is not reported in the site region. Other than minor sedimentary deposition in the center of the Michigan basin (Middle Ionia Formation), no geologic history during the Mesozoic exists in the region of the site (Subsection 2.5.1.1.2.3.2). No evidence of paleoliquefaction is reported in the literature or was observed within the site vicinity or site region. Quaternary cover consists of glacial till and overlying lacustrine sediments of late Wisconsinan age (approximately 13,000 yr BP, Subsection 2.5.1.1.2.3.4.4). No geomorphic expression of deformation of the broad, lacustrine plain overlying mapped or postulated faults in the site vicinity was observed during field or aerial reconnaissance.

2.5.3.5 Relationship of Tectonic Structures in the Site Area to Regional Tectonic Structures

Second-order fold deformation of Silurian and Devonian age bedrock is recognized and documented at the Fermi 3 site. The exact timing of this deformation is not known, but it is likely that it occurred concurrently with

deformation on other related northwest-trending plunging structures in the southeastern part of the Michigan Basin that are referred to as the Washtenaw anticlinorium structures (including the Howell anticline/fault structure). In the Washtenaw anticlinorium region folding is recognized in Ordovician through late Mississippian bedrock units (Reference 2.5.3-202, Reference 2.5.3-203). This series of folds along the southeastern margin of the Michigan Basin spatially coincides with the Mid-Michigan gravity high (MGA), which is associated with a Precambrian basement rift zone, the Midcontinent rift system (Figure 2.5.1-220).

2.5.3.6 Characterization of Capable Tectonic Sources

A “capable tectonic source,” as defined by Regulatory Guide 1.208, is described by at least one of the following characteristics:

- Presence of surface or near-surface deformation of landforms or geologic deposits of a recurring nature within the last approximately 500,000 years, or at least once in the last approximately 50,000 years.
- A reasonable association with one or more moderate to large earthquakes or sustained earthquake activity that are usually accompanied by significant surface deformation.
- Structural association with a capable tectonic source having characteristics of either of the above two bullets, such that movement on one could be reasonably expected to be accompanied by movement on the other.

None of the mapped bedrock faults within a 40-km (25-mi) radius or lineaments within an 8-km (5-mi) radius of the Fermi 3 site is assessed to be a capable tectonic source. This conclusion is based on the lack of evidence for post-Mesozoic deformation (e.g., documented paleoliquefaction or post-glacial tectonic deformation) in the site region (Subsection 2.5.3.4), the absence of moderate to large earthquakes or alignments of seismicity in the site vicinity (Subsection 2.5.3.3), and the absence of evidence for Quaternary deformation in the site area (Subsection 2.5.3.1).

2.5.3.7 Designation of Zones of Quaternary Deformation

No zones of Quaternary deformation that would require additional investigation are identified within the Fermi 3 site region.

2.5.3.8 Potential for Surface Deformation at the Site

2.5.3.8.1 Potential for Tectonic Surface Deformation at the Site

The potential for tectonic deformation at the Fermi 3 site is negligible. There are no capable tectonic faults within the site vicinity.

2.5.3.8.2 Potential for Nontectonic Surface Deformation at the Site

The potential for nontectonic deformation at the Fermi 3 site is negligible. There is no evidence of nontectonic deformation at the Fermi 3 site in the form of unloading phenomenon (i.e., pop-up features), glacially-induced faulting, salt migration, dissolution or collapse related to karst, or volcanic intrusion.

2.5.3.9 References

2.5.3-201 Detroit Edison Fermi Unit 2 Updated Safety Analysis Report, Revision 14, November 2006.

2.5.3-202 Ells, G.D., “Structures Associated with the Albion-Scipio Oil Field Trend,” Michigan Geological Survey Open-File Report 62-1, 1962.

2.5.3-203 Ells, G.D., “Architecture of the Michigan Basin,” in Stonehouse, H.B., ed., “Studies of the Precambrian of the Michigan Basin,” Michigan Basin Geological Society Field Trip Guidebook, pp. 60 – 88, 1969.

2.5.3-204 Hanson, K. L., K. I. Kelson, M. A. Angell, and W. R. Lettis, “Techniques for Identifying Faults and Determining Their Origins,” NUREG/CR-5503, variously paginated.

2.5.3-205 Faust, T.H., K. Fujita, K.G. Mackey, L.J. Ruff, and R.C. Ensign, “The September 2, 1994 Central Michigan Earthquake,” *Seismological Research Letters*, Vol. 68, No. 3, pp. 460 – 464, 1997.

2.5.3-206 Hansen, M.C., “Earthquakes and Seismic Risk in Ohio,” *Ohio Geology*, Summer 1993.

2.5.3-207 Environmental Systems Research Institute (ESRI), ESRI ArcGIS 9.1, Data & Maps, Media Kit, Redlands, California, 2006.

2.5.3-208 National Aeronautics and Space Administration (NASA)/U.S. Geological Survey (USGS), "SRTM, Shuttle Radar Topography Mission, SRTM 30 data," http://www2.jpl.nasa.gov/srtm/, 2005.

2.5.3-209 National Geophysical Data Center, National Oceanic and Atmospheric Administration (NOAA), "Great Lakes Bathymetry," bathymetric data, www.ngdc.noaa.gov/mgg/greatlakes/greatlakes.html, accessed 17 August 2007.

2.5.3-210 Wollensak, M.S., ed., *Oil and Gas Fields of the Michigan Basin*, Volume 1, Michigan Basin Geological Society, 1969.

2.5.3-211 Wollensak, M.S., ed., *Oil and Gas Fields of the Michigan Basin*, Volume 2, Michigan Basin Geological Society, 1991.

2.5.3-212 Tanglis, C. (comp.), "Surface Faults in the Southwestern District, Southern Ontario," Ontario Geological Survey, 1995.

2.5.3-213 Aangstrom Precision Corporation, Structure Contour Maps, Mt. Pleasant, Michigan, 1989.
(a) Dundee Residual Structure Contour Map, scale 1:600,000.
(b) Dundee Structure Contour Map, scale 1:600,000.
(c) Sunbury Shale Residual Structure Contour Map, scale 1:600,000.
(d) Sunbury Shale Structure Contour Map, scale 1:600,000.
(e) Traverse Limestone Residual Structure Contour Map, scale 1:600,000.
(f) Traverse Limestone Structure Contour Map, scale 1:600,000.

2.5.3-214 Baranoski, M.T., "Structure Contour Map on the Precambrian Unconformity Surface in Ohio and Related Basement Features," Ohio Geological Survey Map PG-23, Columbus, Ohio, scale 1:500,000, with 18-page description, available on CD-ROM, 2002.

2.5.3-215 Michigan Department of Natural Resources, "Quaternary Geology of Michigan," Edition 2.0, digital map, 1998.

2.5.3-216 Ontario Geological Survey, "Quaternary Geology, Seamless Coverage of the Province of Ontario," Data Set 14, 1997.

2.5.3-217 U.S. Geological Survey EROS Data Center, "National Elevation Dataset," http://gisdata.usgs.net/ned/, 1999.

2.5.3-218 Newcombe, R.B., *Oil and Gas Fields of Michigan: A Discussion of Depositional and Structural Features of the Michigan Basin*, Michigan Geological Survey, Publication 38, 1933.

2.5.3-219 U.S. Department of Agriculture (USDA), black- and white-aerial photographs, Monroe County, Michigan, 1:20,000 scale, flown 1955

2.5.3-220 U.S. Department of Agriculture (USDA), Digital Orthophotographs for Monroe, Washtenaw, Wayne Counties, Michigan and Lucas, Ottawa, and Wood Counties, Ohio, 2 m resolution, purchased from http://datagateway.nrcs.usda.gov/, flown 2006.

Figure 2.5.3-201 Map Showing Mapped Structures and Seismicity in the Site Vicinity EF3 COL 2.0-28-A

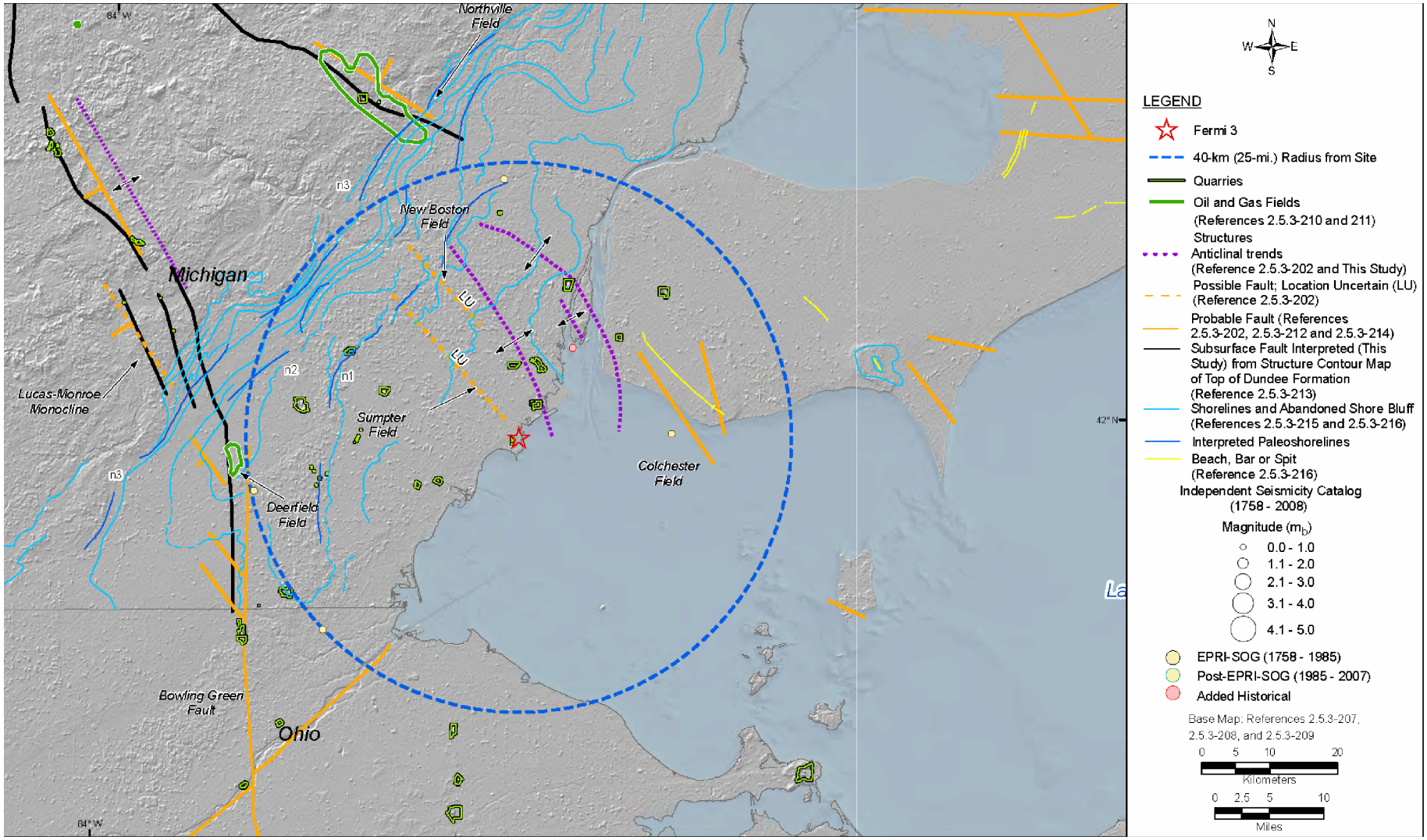

Figure 2.5.3-202 Map Showing Field Reconnaissance Sites, Quarries, and Aerial Reconnaissance Route

EF3 COL 2.0-28-A

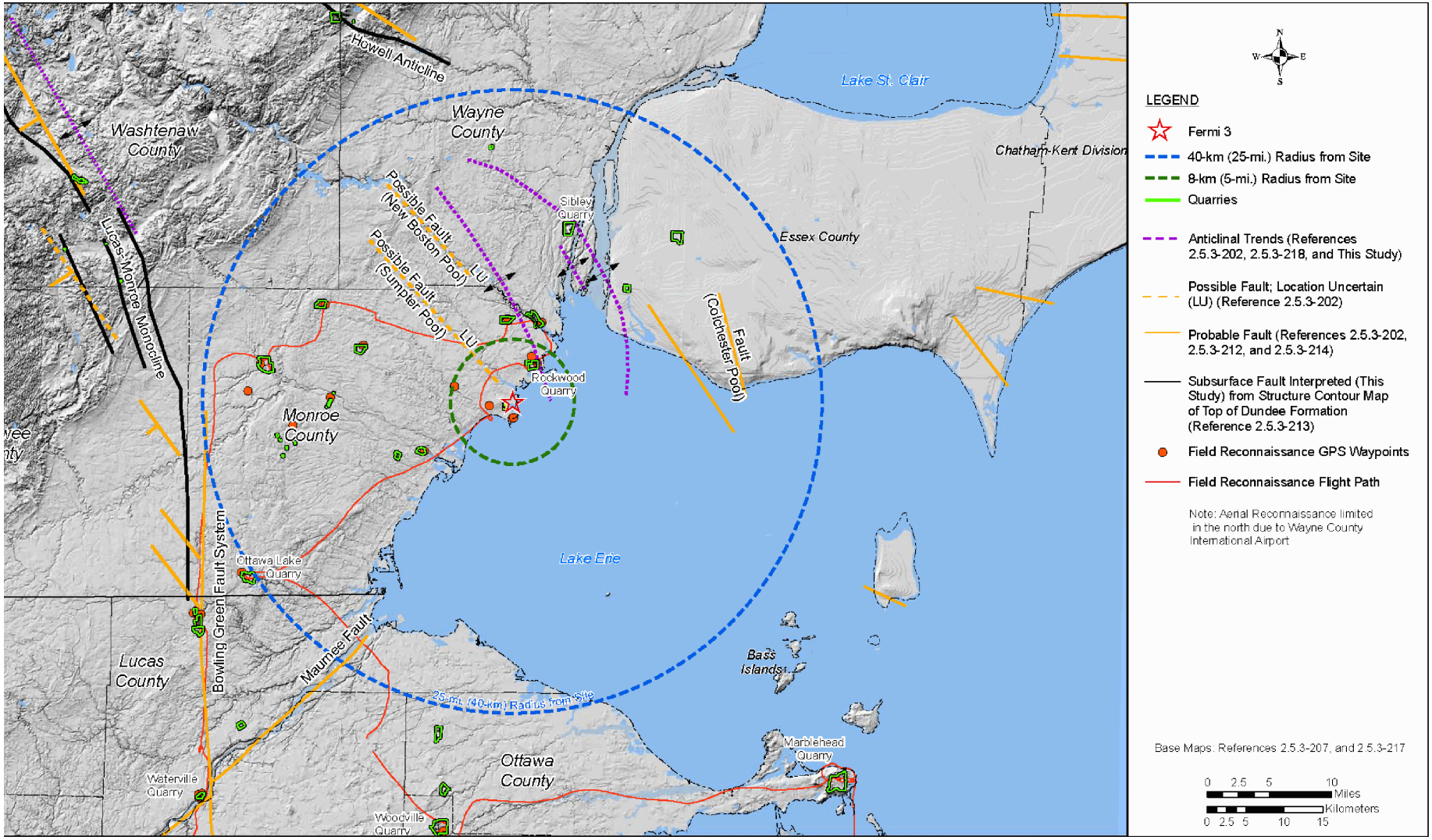

Figure 2.5.3-203 Interpreted Hillshade Model (10-m DEM) Showing Lineaments in the Site Vicinity EF3 COL 2.0-28-A

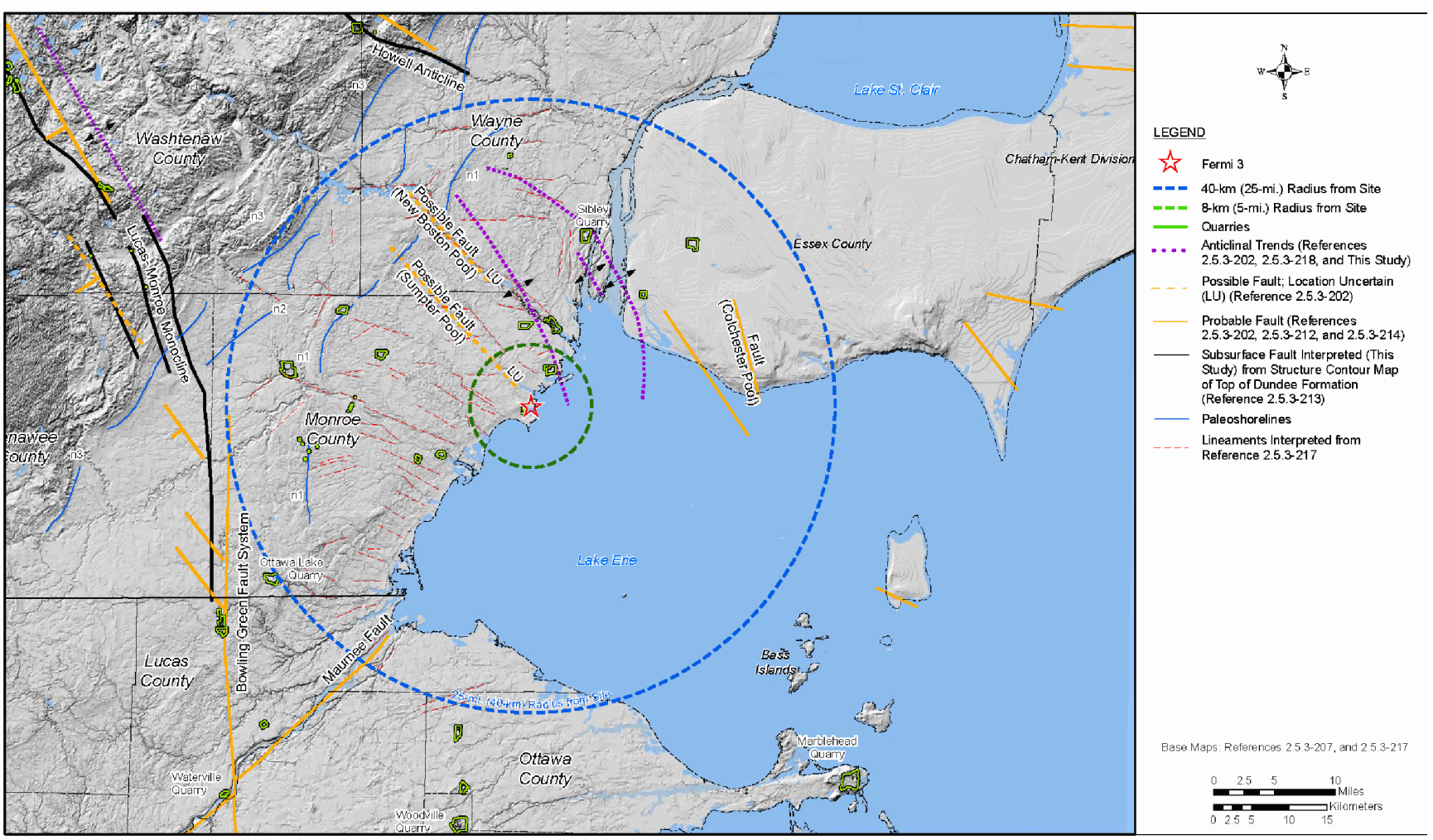

Figure 2.5.3-204 Uninterpreted Hillshade Model (10-m DEM) of the Site Vicinity EF3 COL 2.0-28-A

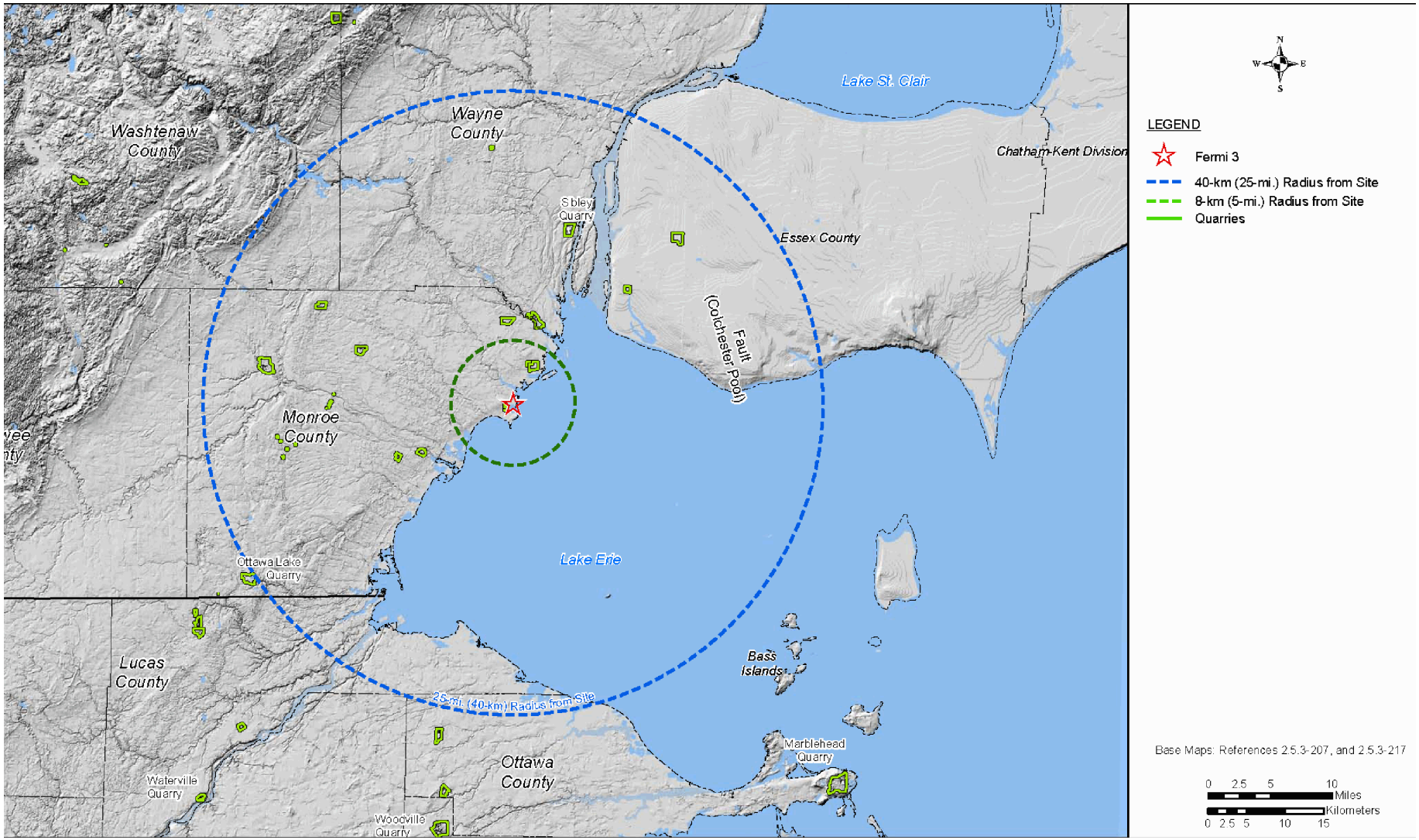

Figure 2.5.3-205 Interpreted 1955 1:20,000-scale Aerial Photograph Mosaic Showing Lineaments in the Site Area

EF3 COL 2.0-28-A

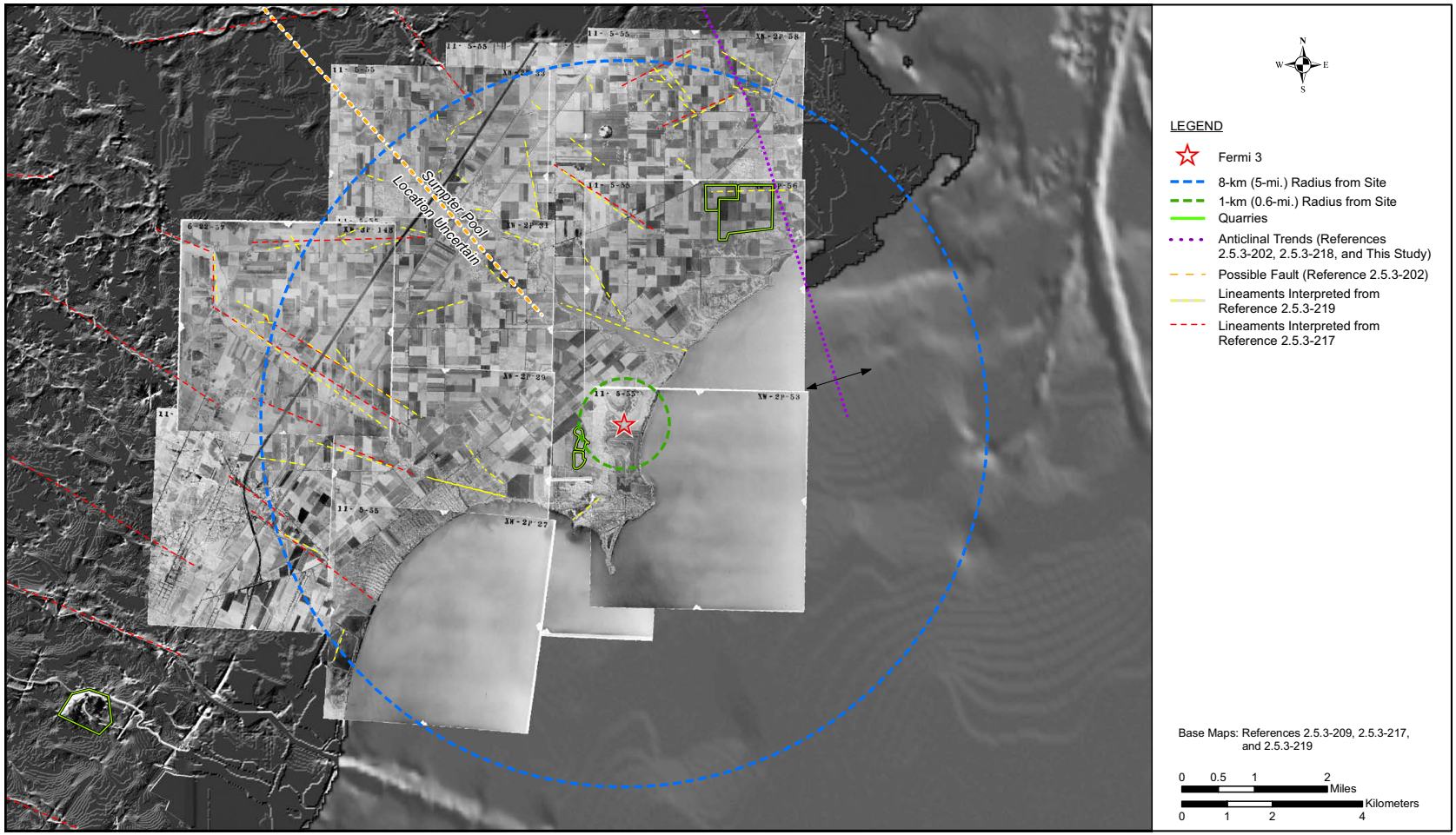

Figure 2.5.3-206 Uninterpreted 1955 1:20,000-scale Aerial Photograph Mosaic of the Site Area EF3 COL 2.0-28-A

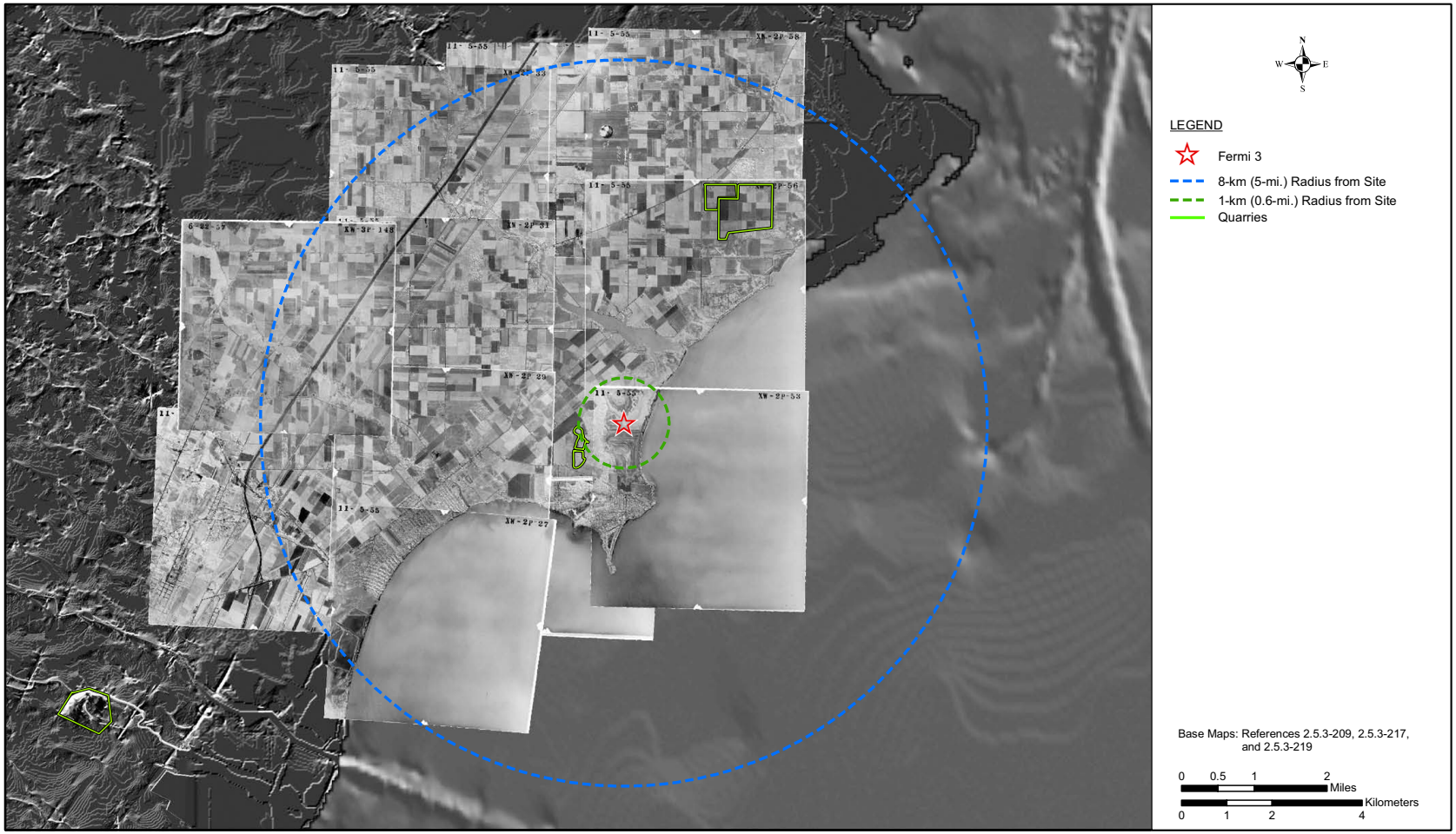

Figure 2.5.3-207 2006 2-m resolution Color Infrared Photograph Showing Interpreted Lineaments in the Site Area

EF3 COL 2.0-28-A

Figure 2.5.3-208 Uninterpreted 2006 2-m resolution Color Infrared Photograph of Site Area EF3 COL 2.0-28-A

Figure 2.5.3-209 Uninterpreted 2006 2-m resolution Color Infrared Photograph of the Site Location EF3 COL 2.0-28-A